DOI: 10.37943/CPJU3187

Ramazan Sadvakassov
Master's Degree, Senior Lecturer, Department of Artificial Intelligence
sadvakasov.rm@gmail.com, orcid.org/0009-0001-8634-1927
L.N. Gumilyov Eurasian National University, Kazakhstan
Kuralay Sadvakassova
Candidate of Pedagogical Sciences, Assistant Professor,
School of Artificial Intelligence and Data Science
sadvakasova.klara65@gmail.com, orcid.org/0009-0003-0130-572X
Astana IT University, Kazakhstan
Togzhan Jumadiyeva
Master's Degree, Independent Researcher
jumadiyeva.t@gmail.com, orcid.org/0009-0001-1928-5873
Astana, Kazakhstan

MULTI-AGENT EVACUATION SIMULATION WITH FIRE AND SMOKE DYNAMICS: A REPRODUCIBLE BASELINE SINGLE-FLOOR STUDY

Abstract: Fire evacuation in buildings is shaped by the interaction between hazard growth, spatial configuration, and heterogeneous occupant behaviour. This study develops a reproducible multi-agent evacuation model in the Mesa framework for hazard-aware analysis under a controlled baseline scenario. The model couples dynamic fire and smoke propagation with four occupant categories: healthy adults, elderly/children, panicking individuals, and leaders. The revised experiment uses a six-room corridor layout with internal partitions, columns, and furniture-like barriers, allowing evacuation performance to be assessed under a more constrained geometry than an open-plan baseline. In the canonical run, the scenario terminates at step 128 with 92 evacuated agents, 8 fatalities, and no remaining active agents. Mean evacuation/removal times differ strongly by agent type: leaders and healthy adults leave earlier on average (19.4 and 29.6 steps), whereas panicking agents (41.9 steps) and elderly agents (56.4 steps) require substantially longer times. Hazard growth is also substantial, with fire reaching 281 cells and smoke saturating all 1200 grid cells by the end of the run. Exit use remains nearly balanced between the two side exits (48 and 44 evacuees), suggesting distributed egress under the assumed navigation rules. Across 30 stochastic runs, the mean evacuation count is 91.9 ± 4.3 agents, mean fatalities are 8.1 ± 4.3, and mean completion time is 131.7 ± 16.0 steps, indicating stable behaviour across random initializations. Sensitivity analysis further shows that the mean evacuation rate declines from 0.955 to 0.854 as fire spread probability increases from 0.04 to 0.15. The model is therefore presented as a transparent comparative baseline, not as a calibrated operational prediction for a specific building.

Keywords: multi-agent simulation, evacuation modeling, fire dynamics, smoke propagation, building safety, agent-based modeling, Mesa framework, emergency management

Introduction

Building evacuation during fire emergencies represents one of the most critical challenges in urban safety engineering, with human casualties often resulting from inadequate evacuation planning rather than direct fire exposure [1]. As cities worldwide experience rapid urbanization and vertical expansion, the complexity of evacuation scenarios has increased dramatically, necessitating sophisticated computational tools to predict and optimize egress strategies. Multi-agent simulation (MAS) has become a widely used approach for modeling evacuation dynamics, enabling researchers to capture the heterogeneous behaviors, decision-making processes, and social interactions that characterize real-world emergency responses [2].

Copyright © 2026, Authors. This is an open access article under the Creative Commons CC BY-NC-ND license
Received: 12.06.2026 Accepted: 17.07.2026 Published: 30.06.2026

Scientific Journal of Astana IT University
ISSN (P): 2707-9031 ISSN (E): 2707-904X
VOLUME 26, JUNE 2026

The capital city of Astana, Kazakhstan, illustrates a broader Central Asian trend of rapid high-rise and mixed-use development that motivates this study; however, site-specific factors are not represented in the present baseline model and are treated as future work rather than as modelled effects.

Despite the growing body of research on agent-based evacuation modelling, directly comparable and openly reproducible studies for Central Asian urban contexts remain limited. The present study addresses this methodological gap with a transparent Mesa-based baseline that combines heterogeneous occupants, evolving hazards, and explicit spatial constraints, and that can later be extended with measured floor plans, Kazakhstan building regulations, and empirical occupant data.

The contribution is therefore positioned at the modelling-workflow level. The article defines the agent rules, hazard-spread algorithms, spatial layout, and experimental protocol; evaluates the resulting baseline through evacuation performance, stochastic robustness, and fire-spread sensitivity; and identifies the assumptions that must be replaced before the model can support building-specific safety assessment.

1. Agent-Based Evacuation Modeling

Agent-based modeling has become a widely used approach for simulating pedestrian evacuation dynamics, offering advantages over traditional macroscopic approaches by explicitly representing individual decision-making, heterogeneous behaviors, and local interactions [3]. Recent systematic reviews identify 134 studies published between 2013-2023, revealing persistent challenges including modeler bias, computational complexity, and data scarcity for calibration and validation [3]. Despite these challenges, agent-based models provide considerable flexibility for exploring "what-if" scenarios and evaluating intervention strategies before implementation. Early work fusing spatial representations with agent-based reasoning established a methodological foundation for indoor dynamic fire-evacuation analysis that recent studies continue to extend [4].

Contemporary evacuation models increasingly incorporate sophisticated pathfinding to navigate complex layouts. Pathfinder has been used for passenger evacuation in subway-train fire scenarios [1], and Fire Dynamics Simulator (FDS) has been coupled with Pathfinder to analyse evacuation in naturally ventilated bifurcated tunnels [5]. These studies highlight the importance of high-fidelity pathfinding that accounts for static obstacles, dynamic hazards, and crowd flow. Cellular-automata approaches have also been refined for exit-selection behaviour, with an improved cellular automata model proposed for exit selection during fire disasters [6] and later extended to dynamic exit selection and counting-area adjustment in asymmetrical layouts [7].

The transition from grid-based to continuous-space models represents a notable methodological development. A social-force-based model for pedestrian evacuation with static guidance was developed to capture realistic crowd phenomena such as bottlenecking and "faster-is-slower" effects [8]. This approach was later extended with a modified social force model incorporating collision-predicting behaviors, enabling agents to anticipate and avoid potential collisions before they occur [9]. These continuous-space models overcome the "checkerboard" movement artifacts inherent in grid-based approaches, producing more realistic evacuation trajectories and time estimates.

2. Fire and Smoke Dynamics Integration

The coupling of agent-based evacuation models with physics-based fire simulations represents a current direction in evacuation safety analysis. FDS (Fire Dynamics Simulator) is widely used for computational fluid dynamics (CFD) modeling of fire environments, providing high-resolution spatiotemporal data on temperature, visibility, and toxic gas concentrations [5]. PyroSim, a graphical user interface for FDS, facilitates the creation of complex building geometries and fire scenarios, enabling researchers to generate realistic hazard fields for evacuation analysis [1]. Complementing these CFD-coupled approaches, an agent-based indoor evacuation simulator has been developed that incorporates fire impacts directly at the agent level without requiring full CFD coupling, an approach methodologically closer to the present study's grid-based baseline [10].

Critical to survivability assessment is the Fractional Effective Dose (FED) metric, which quantifies cumulative toxic exposure from combustion products. Directing evacuees upstream of the fire after detection has been shown to reduce injuries and improve overall evacuation success, as analysed through FED [5].

Smoke effects on evacuation have received increasing attention. Explicitly modelling smoke has been found to increase evacuation-time estimates by approximately 50% relative to models that omit it, highlighting a substantial underestimation risk when smoke propagation is ignored [11]. The importance of accounting for hazard evolution is echoed in other contexts, where evacuation risk has been shown to change over time under accidental toxic-gas releases, reinforcing the principle that evacuation strategy must respond to a dynamically evolving hazard state rather than a static one [12].

Fire spread in high-rise buildings is shaped by vertical propagation. The effect of wind direction on fire spread across high-rise facades has been examined using PyroSim [13], while FDS has been used to study fire spread and protection strategies in brick-timber heritage buildings [14]. High-rise-specific agent-based modelling has also examined post-ignition occupant response, showing that agent-based simulation of high-rise building fires can reveal self-rescue behaviours and inform improved fire-protection design [15].

3. Behavioral Heterogeneity in Evacuation

Recognition of behavioral heterogeneity among evacuees has become a central focus in contemporary evacuation modeling. Building evacuation efficiency has been enhanced by integrating evacuee categorization into agent-based simulation, differentiating agents by environmental knowledge (staff vs. visitors) and mobility constraints (able-bodied vs. mobility-impaired) [2]. This categorization was shown to improve representational detail, with familiar agents (staff) exhibiting faster evacuation times and more efficient route selection compared to unfamiliar visitors. An earlier precedent for this behavioural-spatial integration combined human-behaviour modelling with predictable spatial accessibility analysis for building evacuation in a fire emergency [16].

Age-related differences in evacuation behavior have been extensively documented. A simulation-based method for optimal building evacuation planning has been developed specifically focused on emergency behavior among older adults [17]. This work found that elderly evacuees exhibit slower movement speeds, longer decision-making times, and greater susceptibility to environmental stressors such as smoke and heat. Evacuation time has similarly been reported to increase with higher proportions of older people and children in the evacuating population, emphasizing the need for age-stratified evacuation planning [1].

Leadership and guidance mechanisms significantly influence evacuation outcomes, particularly in complex or unfamiliar environments. Leader agents and static guidance have been incorporated into a social force-based evacuation model, demonstrating that trained personnel can improve evacuation efficiency by approximately 35% through real-time information provision and crowd management [8]. Agent-based simulation of crowd evacuation through complex spaces has also been examined, highlighting the importance of situational awareness and dynamic guidance systems in reducing evacuation times and preventing bottlenecks [18]. At the system level, a coupled simulation-optimization model for evacuation guidance planning has been proposed, illustrating how leader-driven guidance can be formally optimised rather than only simulated at the individual-agent level [19].

Panic behavior represents a critical but challenging aspect of evacuation modeling. While panic is often cited as a major factor in evacuation failures, empirical evidence suggests that true panic (characterized by irrational, self-destructive behavior) is relatively rare. Instead, evacuees typically exhibit "adaptive" behaviors that may appear panicked but are actually rational responses

Scientific Journal of Astana IT University
ISSN (P): 2707-9031 ISSN (E): 2707-904X
VOLUME 26, JUNE 2026

to perceived threats [20]. Modeling panic requires careful consideration of psychological factors, social influence, and information availability, areas that remain underexplored in current literature.

4. Regional Context: Central Asian Building Safety

Despite the extensive global literature on evacuation modelling, studies that specifically address Central Asian urban contexts remain limited. Publicly visible and methodologically comparable studies for the region are few, indicating a geographic transferability gap. This gap is relevant given the rapid urbanization and high-rise construction throughout the region.

The literature search used in this article should be interpreted as a targeted narrative review rather than a full systematic review. The search focused on recent evacuation, fire, smoke, and agent-based simulation studies, with additional attention to works mentioning Kazakhstan, Astana, and Central Asian urban contexts. Since no formal PRISMA-style protocol was applied, the claim is formulated cautiously: directly comparable and publicly visible evacuation-simulation studies for Central Asian building contexts appear limited, rather than entirely absent.

Locally calibrated evacuation data for Astana and comparable Central Asian cities remain scarce. Region-specific building practices and occupant characteristics have been discussed qualitatively in the fire-safety literature but are not yet systematically integrated into evacuation models; they fall outside the present two-dimensional baseline and are revisited as future work.

Modern high-rise and mixed-use developments in the region combine residential, commercial, and office spaces, producing diverse occupant populations with varying building familiarity and mobility. Such layouts can affect smoke movement and route choice in ways that a generic single-floor model does not capture, which is one reason the present study is framed as a baseline rather than a building-specific assessment.

This literature review reveals a narrower set of gaps addressed in the present article: the need for a transparent hazard-coupled baseline model, explicit treatment of heterogeneous agents, and clearer separation between demonstrated results and future region-specific calibration. The following methodology section describes the corresponding baseline framework.

To clarify the methodological position of the present study, Table 1 compares selected evacuation simulation approaches across model class, hazard representation, agent heterogeneity, pathfinding logic, and validation strategy. The comparison highlights the trade-off between physical fidelity, behavioral detail, reproducibility, and data requirements; in this context, CFD refers to Computational Fluid Dynamics, FDS to Fire Dynamics Simulator, and CA to Cellular Automaton. The present study is positioned as a transparent and reproducible open-source baseline, with its main limitation being the absence of CFD coupling and empirical validation against real evacuation data.

Table 1. Critical comparison of selected agent-based evacuation models

Study	**Model Class**	**Hazard Model**	**Agent Types**	**Pathfinding**	**Validation**
Present study	Grid ABM (Mesa)	Stochastic CA (fire + smoke)	4 types (healthy, elderly, panic, leader)	Nearest-exit selection + A* shortest safe grid path	Face validity + ratio-level comparison
Wang et al. [1]	Continuous (Pathfinder)	CFD (FDS)	Homogeneous	Pathfinder	Empirical (subway)
Chen et al. [5]	Continuous (Pathfinder)	CFD (FDS/FED)	Homogeneous	Pathfinder	Empirical (tunnel)
Zhang et al [8]	Continuous (Social Force)	None	2 types (leader / follower)	Social force	Face validity

Kasareka et al. [2]	Grid ABM	None	4 types (staff/visitor × mobility)	Shortest path	Face validity
Jha et al. [11]	Continuous	Smoke model	Homogeneous	–	Empirical (hospital)

The comparison shows that high-fidelity evacuation studies often rely on specialized tools such as FDS, Pathfinder, or social-force-based models, which provide more realistic physical or crowd-dynamic representation but require detailed geometry, calibration data, and greater modeling effort. In contrast, grid-based agent-based models provide lower physical realism but offer transparency, reproducibility, and flexibility for testing behavioral assumptions. The present study is therefore positioned as a reproducible hazard-coupled baseline: it combines heterogeneous agents with simplified fire and smoke propagation in one consistent simulation workflow, while explicitly acknowledging the absence of CFD coupling and empirical validation.

Methods and Materials

1. Model Architecture and Framework

The evacuation simulation model was implemented using the Mesa agent-based modeling framework (version 3.5.0), a Python-based platform that provides flexible tools for creating, analyzing, and visualizing agent-based models. Mesa was selected for its modular architecture, extensive documentation, and active developer community, making it well-suited for complex evacuation scenarios requiring custom agent behaviors and environmental dynamics [3].

The model combines four interacting elements: a two-dimensional grid environment, heterogeneous occupants, dynamic fire and smoke fields, and static spatial constraints such as exits, partitions, columns, and obstacles. The environment is implemented as a 40 × 30 Mesa MultiGrid (1200 cells). Under the assumed 0.5 m × 0.5 m cell size, this corresponds to a 20 m × 15 m, 300 m² single-floor baseline. The resolution follows standard grid discretisation used in pedestrian cellular-automata models [21-22] and provides a compromise between computational tractability and the spatial detail needed to represent corridor access, doorway openings, and hazard propagation.

The model employs a discrete-time simulation approach with synchronous updating, where all agents and environmental processes execute one step per time unit. Simulation time is reported in model-step units; the present study does not impose a validated one-step-to-one-second calibration. The simulation continues until all agents have either successfully evacuated or perished in the fire, or until a maximum of 500 steps is reached to prevent infinite loops in pathological scenarios.

Mesa is sufficient for the present study because the objective is not to provide a CFD-accurate fire engineering assessment or a validated building-code compliance tool. Instead, the purpose is to create a transparent and reproducible baseline for testing how heterogeneous agents interact with simplified dynamic fire and smoke hazards. Mesa supports explicit agent-level rules, grid-based spatial representation, reproducible random seeds, and straightforward collection of evacuation, hazard, and density metrics. Therefore, it is appropriate for the baseline methodological scope of this article, while more physically accurate extensions would require coupling with FDS, Pathfinder, or other specialized evacuation and fire-simulation platforms.

2. Agent Types and Behavioral Parameters

The model implements four distinct agent types, each characterized by unique behavioral parameters that influence movement speed, visibility range, and decision-making processes. This heterogeneous agent approach aligns with recent literature emphasizing the importance of evacuee categorization for realistic evacuation modeling [2].

The effective movement speed of each agent is determined by the base walking speed and a behavioral multiplier associated with the agent type and environmental conditions. In the model, the effective speed of agent i is defined as:

Scientific Journal of Astana IT University
ISSN (P): 2707-9031 ISSN (E): 2707-904X
VOLUME 26, JUNE 2026

$$v_i = v_{\{base\}} * m_i * s_i \tag{1}$$

Where v_i represents the effective movement speed of agent i, $v_{\{base\}}$ is the baseline walking speed, m_i is the behavioral multiplier associated with the agent type, and s_i represents environmental modifiers such as smoke influence or reduced visibility. This formulation allows the model to capture heterogeneous mobility patterns among different evacuee categories.

Healthy Adults represent the baseline agent type, comprising 60% of the simulated population. These agents use the baseline movement parameter of 1 cell per step before environmental modifiers and type-specific effects are applied. Healthy adults have a visibility range of 20 cells, representing their ability to identify and navigate toward distant exits under normal conditions. Their movement probability is set to 1.0, meaning they attempt to move every simulation step.

Elderly/Children agents represent individuals with reduced mobility and slower decision-making, comprising 20% of the population. These agents have a speed multiplier of 0.5 applied to the base speed, resulting in reduced effective movement relative to the baseline parameter. This reduction reflects empirical findings that elderly evacuees and children move approximately 50% slower than healthy adults during emergencies [17]. Their visibility range is reduced to 15 cells, representing potential visual impairments or reduced situational awareness. Evacuation time has been shown to increase significantly with higher proportions of elderly individuals and children, validating the importance of this agent category [1].

Panicking Agents represent individuals experiencing acute stress responses that impair rational decision-making, comprising 15% of the population. These agents have a speed multiplier of 1.2, reflecting the tendency of panicked individuals to move faster but less efficiently. Their visibility range is substantially reduced to 8 cells, representing tunnel vision and impaired situational awareness characteristic of panic states. Critically, panicking agents have a 30% probability of making random movements rather than following optimal paths toward exits, simulating disorientation and irrational behavior observed in high-stress evacuation scenarios [20].

Leader Agents represent trained personnel such as security staff, fire wardens, or building managers who possess superior knowledge of the building layout and evacuation procedures, comprising 5% of the population. Leaders have a speed multiplier of 1.0 (baseline speed) but an extended visibility range of 25 cells, representing their familiarity with the building and ability to identify optimal evacuation routes. Leader agents follow deterministic pathfinding without random deviations, consistent with their training and experience. This leadership benefit has been quantified at ~35%, supporting the inclusion of this agent type [8].

3. Fire and Smoke Spread Algorithms

The model implements coupled fire and smoke propagation systems that dynamically alter the evacuation environment over time. While simplified compared to full CFD simulations using FDS or PyroSim [5], the algorithms capture essential dynamics of hazard spread and their impact on agent behavior.

Fire Propagation: Fire is initiated at one or more source locations specified in the simulation configuration. Each fire cell has an intensity parameter (ranging from 0.0 to 1.0) and a spread probability parameter (canonical value: 0.08 per step). During each simulation step, fire attempts to spread to adjacent cells (using von Neumann neighborhood: up, down, left, right). The spread probability determines the likelihood of ignition in neighboring cells. The probability of fire propagation can be expressed as:

$$P_{\{spread\}} = \beta * \mathrm{I}_t \tag{2}$$

When fire spreads to a new cell, its intensity is reduced by 10% (multiplied by 0.9), representing energy dissipation and fuel consumption. The fire intensity decay after propagation can be expressed as:

$$I_{\{t+1\}} = 0.9 * I_t \tag{3}$$

Fire does not spread to cells containing obstacles, and multiple fire agents do not accumulate in the same cell. Agents occupying cells that ignite are immediately marked as casualties and removed from the simulation, consistent with the assumption that direct fire exposure is rapidly fatal [1].

Smoke Propagation: Smoke is generated adjacent to fire sources and spreads more rapidly than fire itself, reflecting the physical reality that smoke propagates through convection and diffusion faster than flame fronts [11]. Smoke agents have a density parameter (0.0 to 1.0) and a spread rate parameter (default: 0.15 per step). Smoke spreads using Moore neighborhood (all 8 adjacent cells), enabling diagonal propagation. The evolution of smoke density over time can be approximated as:

$$S_{\{t+1\}} = \alpha * S_t \tag{4}$$

When smoke spreads to a new cell, its density is reduced by 20% (multiplied by 0.8), representing dilution and dispersion. Smoke does not directly kill agents but significantly impairs their movement: agents in smoke-filled cells have their effective speed reduced by 50%, consistent with empirical findings that smoke reduces visibility and causes disorientation [11].

This reduction can be expressed as:

$$v_i^{\{smoke\}} = 0.5 * v_i \tag{5}$$

The fire and smoke algorithms execute before agent movement in each simulation step, ensuring that agents respond to the current hazard state. This sequencing reflects the reality that environmental conditions evolve continuously during evacuations, requiring agents to adapt their strategies dynamically [5].

4. Pathfinding and Movement Logic

Agent navigation is specified as a two-stage process. Each agent first selects a target exit using Manhattan distance subject to visibility constraints. Route execution is then computed by an obstacle-aware A* search over the four-neighbourhood, restricted to cells that are not occupied by obstacles or fire. This formulation is required by the revised corridor-room geometry: continuous internal partitions and explicit doorway openings make direct greedy movement inappropriate because feasible movement depends on passage connectivity rather than Euclidean proximity alone.

For each agent at position (x, y), the algorithm computes the Manhattan distance to each exit:

$$d = | x_{\{exit\}} - x_{\{agent\}} | + | y_{\{exit\}} - y_{\{agent\}} | \tag{6}$$

The agent selects the exit with minimum distance as its target. However, agent type influences this selection: healthy adults, elderly, and leaders consider all exits within their visibility range, while panicking agents have reduced visibility and may not perceive distant exits. This visibility-based exit selection captures the realistic constraint that evacuees can only navigate toward exits they are aware of [8].

Scientific Journal of Astana IT University
ISSN (P): 2707-9031 ISSN (E): 2707-904X
VOLUME 26, JUNE 2026

After the target exit and path are determined, movement follows the next available cell along the A* route. The distance advanced in each step is controlled by the agent's effective speed, which depends on agent type and smoke exposure. Fractional movement speeds are accumulated across steps so that slower agents, especially elderly occupants or agents crossing smoke-filled cells, retain their intended relative mobility over time.

Collision avoidance is handled during path expansion and movement execution. Cells containing obstacles or fire are excluded from planned routes, and occupied cells are checked before movement. When no safe path is available, the agent selects a locally safe adjacent cell that reduces distance to the target where possible. The rule is intentionally simpler than social-force formulations, but it prevents the artificial wall-crossing behaviour that would otherwise occur in the partitioned layout.

5. Simulation Parameters and Experimental Design

The simulation experiments employed the following parameters, selected to define a controlled baseline single-floor evacuation scenario motivated by common building-safety concerns, rather than a calibrated representation of a specific Astana building:

- Grid dimensions: 40 × 30 cells (1200 cells total); each cell represents a 0.5 m × 0.5 m area (standard grid discretization; see [21, 22]), yielding a floor area of 20 m × 15 m = 300 m²
- Number of agents: 100 (initial occupant load)
- Agent distribution: 60% healthy, 20% elderly, 15% panic, 5% leader
- Number of exits: 2, located at (0, 15) and (39, 15), centred on the left and right external walls
- Number of obstacles: 170 cells; two horizontal internal partitions form a central corridor with three doorway openings on each side, while room-separating partitions, six regularly spaced structural columns, and furniture-like barriers define the internal layout. The geometry is a generic single-floor baseline and is not a calibrated real building plan.
- Fire source: 1 initial ignition point (x = 20, y = 8), placed in the lower-central office zone to create a single controlled hazard origin
- Fire spread probability: 0.08 per step
- Smoke spread rate: 0.15 per step
- Base agent speed: 1 cell/step before modifiers
- Movement probability: 0.8

Table 2. Model parameter justification

Parameter	Value	Justification / Source
Cell size	0.5 m × 0.5 m	Standard grid discretization in pedestrian CA models [21, 22]
Floor area	300 m² (40 × 30 × 0.25)	Derived from cell size; consistent with residential/office floor scale [21]
Occupant density	0.33 pers/m² (100 / 300)	Pre-emergency occupancy; density–velocity coupling [23, 24]
Healthy speed (1.0×)	~0.5 m/step	Used as a relative mobility parameter; model steps are not calibrated to real seconds. Literature speeds motivate relative differences only [25, 26].
Elderly speed (0.5×)	~0.25 m/step	0.5–0.8 m/s; reduced mobility of elderly/children [25, 27]
Panic speed (1.2×)	~0.6 m/step	Elevated speed but impaired navigation [20]
Panic proportion (15%)	0.15	Observed range 10–20% in real evacuations [20]
Fire spread prob.	0.08 per step	Calibrated to realistic spread; CA fire benchmark [22]; sensitivity 0.04–0.15 (this study)

Smoke spread rate	0.15 per step	Smoke travels 2–3× faster than the fire front [11]
Simulation steps	500 max	Sufficient for simulation completion in all 30 stochastic runs.

- Maximum simulation steps: 500 model steps

The canonical scenario is reported for seed = 42. Stochastic robustness is evaluated through 30 additional runs with seeds 1-30 while holding all model parameters fixed. To examine parameter sensitivity, fire spread probability is varied from 0.04 to 0.15, with 10 stochastic runs for each value. These supplementary experiments separate layout-dependent behaviour in the baseline run from variability caused by random initialization and hazard spread.

Data analysis was performed using Python scientific computing libraries (NumPy, Pandas, Matplotlib, Seaborn). Statistical summaries include mean, median, standard deviation, and range for key metrics. Visualizations were generated to illustrate cumulative evacuation patterns, time distributions, exit utilization, hazard spread dynamics, agent performance comparisons, spatial density heatmaps, and multi-metric timelines.

Results

1. Cumulative Evacuation Patterns

The cumulative evacuation curve in Figure 1 retains an S-shaped profile, but the revised corridor-room layout slows the process relative to the earlier open-plan geometry. Only 4 agents have evacuated by step 10; evacuation then accelerates as agents reach the corridor and exits, passing the 50% mark at step 25. The run terminates at step 128 with 92 evacuated agents, 8 fatalities, and no remaining active agents.

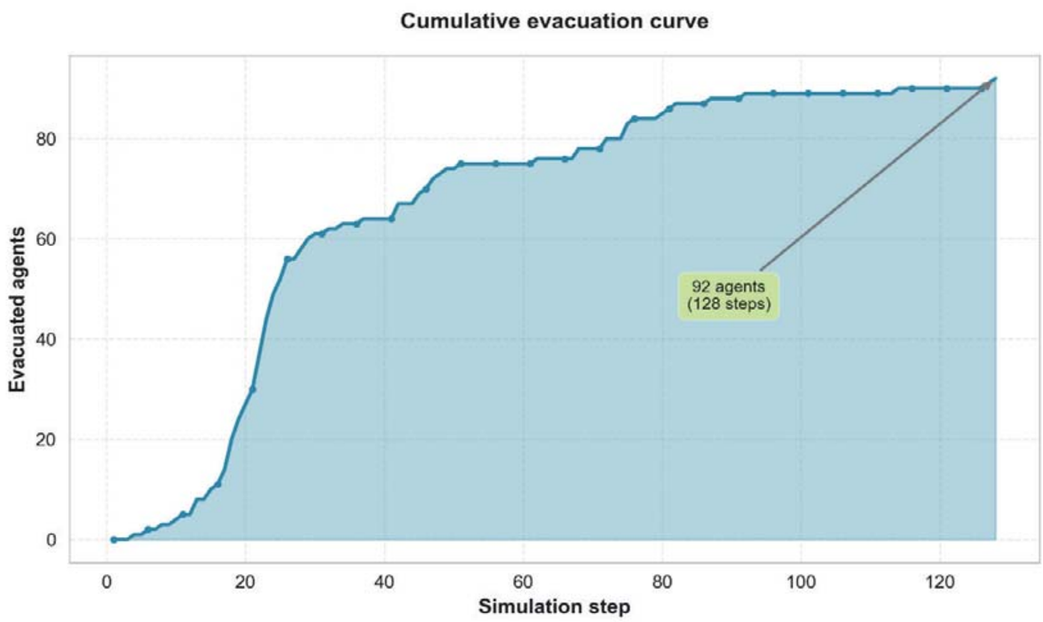

Figure 1. Cumulative evacuated agents over simulation time for the revised six-room corridor layout

The early phase (steps 1-10) is deliberately slow in the revised geometry: only 4 agents (4%) evacuate before the corridor flow becomes established. This reflects the combination of interior starting positions, room-door access constraints, and still-developing hazard fields.

The main acceleration occurs between steps 11 and 25, as agents reach the corridor and the side exits; the first fatalities also appear within this window, so hazard exposure begins to affect outcomes before half of the population has reached safety. The absence of severe exit congestion

Scientific Journal of Astana IT University
ISSN (P): 2707-9031 ISSN (E): 2707-904X
VOLUME 26, JUNE 2026

suggests that the three doorway openings on each corridor side provide sufficient local access at this baseline density.

After step 25, evacuation enters a long terminal phase. The remaining 45 active agents are disproportionately affected by reduced mobility, panic-induced route inefficiency, longer initial distances, or exposure to expanding smoke and fire. The final outcome consists of 40 additional evacuations and 5 additional fatalities, producing 92 evacuees and 8 deaths by step 128.

2. Evacuation Time Distribution Analysis

Figure 2 summarises individual evacuation or removal times for all 100 agents. The distribution is strongly right-skewed: the mean is approximately 36.3 steps, the median is 24 steps, and the longest observed removal time reaches step 128. The delayed tail is consistent with the combined effect of room-corridor routing, furniture barriers, slower elderly agents, panic-driven deviations, and progressive hazard exposure.

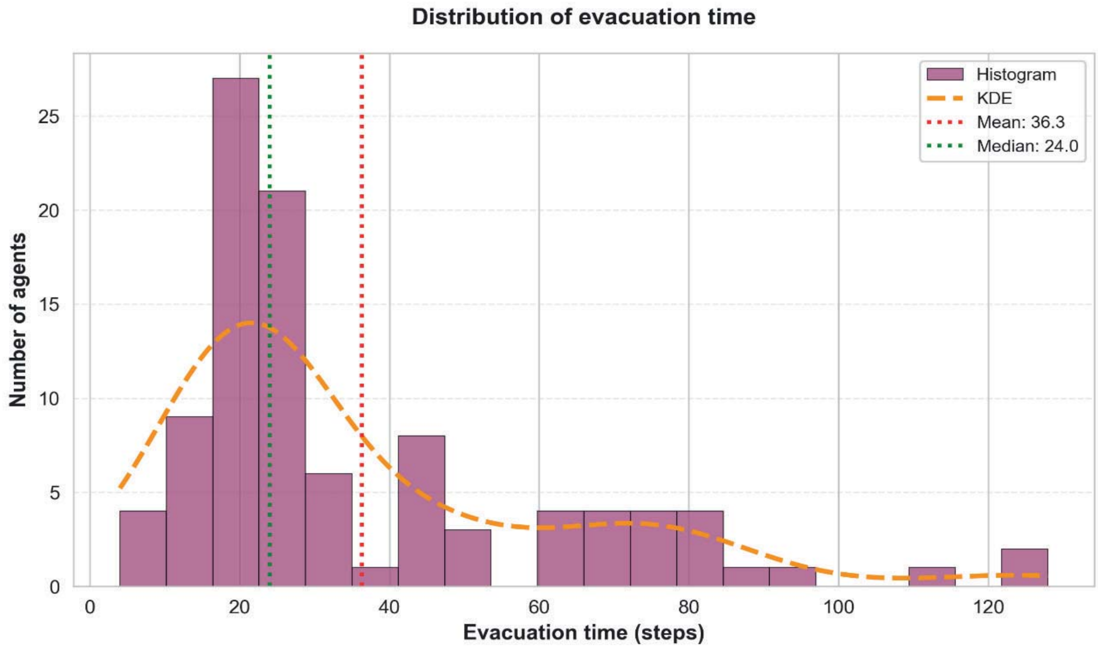

Figure 2. Distribution of evacuation/removal times for all agents

The shortest evacuation times correspond to agents initially located near the side exits or already positioned close to the central corridor. Most removals occur after agents have traversed room-door connections and joined the main corridor flow, making initial placement and local access constraints central determinants of the distribution.

The long tail is dominated by elderly and panicking agents. Elderly agents are slowed by the 0.5 speed multiplier, so equivalent path lengths require more simulation steps. Panicking agents may take less efficient routes because random movement interrupts otherwise shortest-path navigation, increasing both travel distance and exposure time.

For planning interpretation, the median alone is insufficient. Although half of the agents are removed by approximately step 24, a substantial minority remains exposed for much longer. This pattern supports treating vulnerable occupants explicitly in evacuation models rather than representing the population by a single average walking speed.

3. Exit Utilization and Load Balancing

Table 3 reports how the evacuated agents are distributed between the two configured exits. The near-balanced split reflects the nearest-exit selection rule operating within a symmetric side-exit layout.

Table 3. Number and share of agents evacuating through each of the two building exits (baseline run, seed = 42; total evacuated = 92)

Exit	Location	Agents evacuated	Share
Exit 1	(0, 15)	48	52.2%
Exit 2	(39, 15)	44	47.8%
Total	–	92	100%

The near-balanced 48/44 split suggests that no single exit became the dominant bottleneck in the canonical scenario. This contrasts with some real-world evacuation scenarios where familiarity bias causes evacuees to preferentially use main entrances even when alternative exits are closer, leading to dangerous congestion [2].

Exit-flow analysis shows that the maximum instantaneous flow through any exit did not exceed 3 agents per model step. Because the model is not calibrated to real seconds or physical doorway width, this value should be interpreted only as a relative simulation metric rather than a direct comparison with engineering capacity standards. Under the baseline assumptions, no severe exit-level congestion was observed; however, in higher-density scenarios or geometries with fewer exits, exit flow could become a limiting factor requiring further scenario-specific analysis.

4. Fire and Smoke Spread Dynamics

Figure 3 traces the coupled growth of fire and smoke during the baseline run. Fire expands from one ignition cell to 281 cells by step 128, whereas smoke spreads more rapidly and eventually covers all 1200 grid cells.

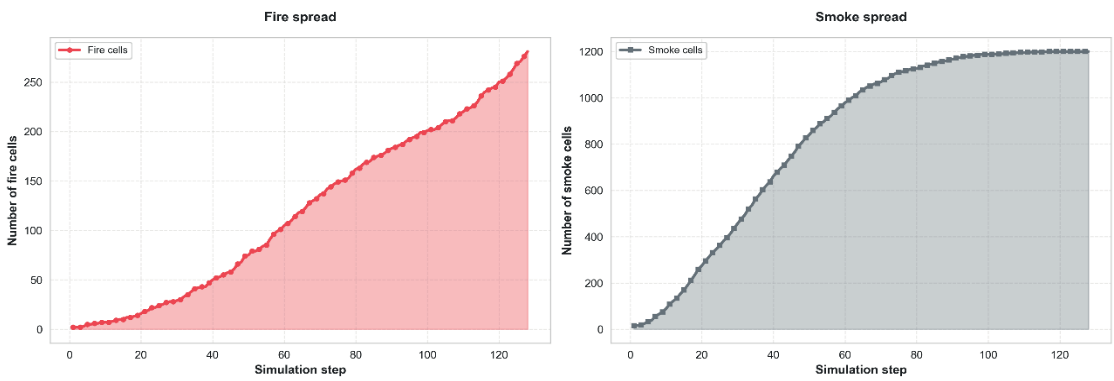

Figure 3. Temporal evolution of fire cells and smoke cells

Fire growth remains stochastic throughout the run and slows as the front encounters obstacles, partitions, and grid boundaries. By the final step, fire occupies approximately 23.4% of the grid. Most successful evacuations occur before this final hazard state, underscoring the importance of early corridor access and short route completion times.

Smoke outpaces fire because the smoke probability parameter is higher (0.15 versus 0.08) and diffusion uses the Moore neighbourhood rather than the von Neumann neighbourhood. This modelling choice reflects the broader evacuation risk posed by smoke: it can affect mobility and survivability even when direct flame contact remains spatially limited.

By step 10, smoke has reached 89 cells (7.4% of the grid), and by step 20 it has expanded to 275 cells (22.9%). Agents crossing smoke-filled areas experience a 50% speed reduction, reducing healthy-adult movement to 0.5 cells per step and elderly movement to 0.25 cells per step. This impairment mechanism is consistent with the smoke benchmark discussed in Section 2 [11], while remaining an abstract mobility parameter rather than a calibrated toxicological prediction.

The spatial pattern of smoke spread indicates directional asymmetry within the two-dimensional grid. In real buildings, vertical smoke movement would require a dedicated three-dimensional or multi-floor model. Therefore, the present result should be interpreted as a

Scientific Journal of Astana IT University
ISSN (P): 2707-9031 ISSN (E): 2707-904X
VOLUME 26, JUNE 2026

simplified two-dimensional hazard-spread pattern rather than as a representation of vertical smoke dynamics.

5. Agent Type Performance Comparison

Figure 4 compares evacuation/removal times by agent type. The ordering follows the behavioural assumptions of the model: leaders are fastest on average (19.4 steps), followed by healthy adults (29.6), panicking agents (41.9), and elderly agents (56.4).

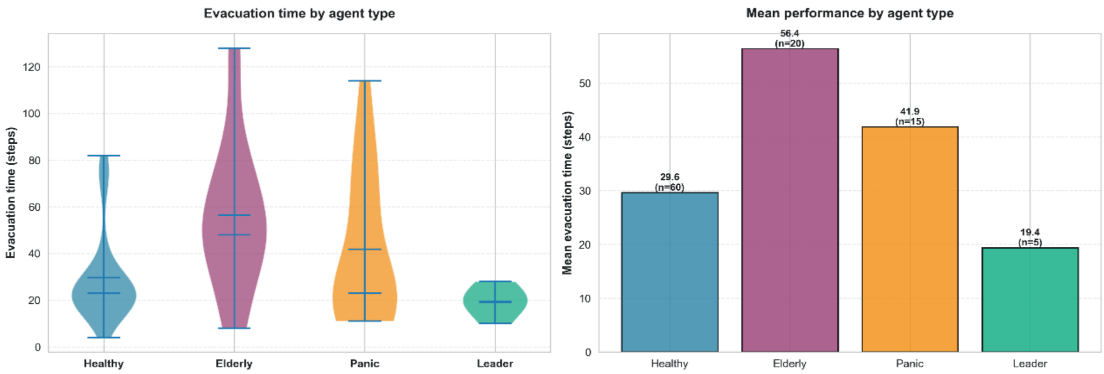

Figure 4. Evacuation/removal times by agent type

Leaders form the fastest cohort in the canonical run, with a mean removal time of 19.4 steps. Their advantage is attributable to longer visibility range and deterministic navigation without random deviations, although the small cohort size (n = 5) means that the magnitude of the difference should not be overinterpreted.

Healthy adults establish the main reference group for the population, with a mean removal time of 29.6 steps. The observed dispersion (SD = 19.4 steps) is driven by initial position, room-door access, and local exposure to fire or smoke rather than by behavioural randomness alone.

Panicking agents show slower and more variable performance, with a mean removal time of 41.9 steps and SD of 32.3 steps. The 30% probability of random movement produces inefficient route segments for some agents, increasing path length and exposure. This result is consistent with the broader treatment of panic as a risk-amplifying factor in evacuation modelling [20].

Elderly agents have the longest mean removal time (56.4 steps; SD = 32.6), approximately twice that of healthy adults. The difference follows directly from the 0.5 speed multiplier and illustrates how vulnerable groups can determine the late-stage evacuation profile even when average population performance appears acceptable.

6. Spatial Density Heatmap Analysis

Figure 5 presents a spatial heatmap showing the cumulative density of agent positions throughout the simulation, revealing high-traffic corridors, congestion points, and evacuation flow patterns. The heatmap is normalized to show relative density, with warmer colors (red/orange) indicating high-traffic areas and cooler colors (blue) indicating low-traffic areas.

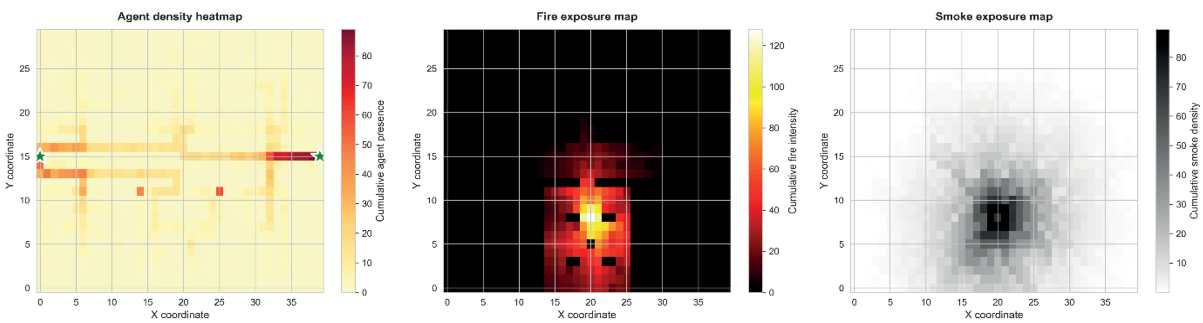

Figure 5. Spatial heatmap showing cumulative agent density throughout the simulation

The heatmap reveals two dominant high-density corridors extending from the central building area toward the two exits, representing the primary evacuation routes. The spatial crowd density within the grid can be defined as the ratio between the number of agents and the corresponding area:

$$\rho = \frac{N}{A} \tag{7}$$

Where ρ is the crowd density, N is the number of agents within the observed region, and A is the corresponding spatial area.

These corridors exhibit peak densities 3-4 times higher than the building average, indicating that most agents followed similar optimal paths toward their nearest exits. The corridor pattern validates the pathfinding logic, as agents successfully identified and followed shortest-path routes.

The central region shows moderate, fairly uniform density from the initial agent placement, while low-density zones at the corners and along obstacle-blocked edges act as dead space outside the main routes. Most of the floor area nonetheless contributes to evacuation flow rather than remaining inaccessible.

The heatmap does not indicate severe bottleneck formation. Peak density is only about three to four times the average level, which is consistent with the balanced exit utilisation in Table 3 and with the absence of sustained exit queues in the baseline run. Higher occupant density, narrower doors, or asymmetric exit placement would likely produce a different pattern and should be tested separately before drawing design conclusions.

Figure 6 illustrates the spatial process behind the aggregate curves. Agents begin distributed across six rooms and the central corridor, then move through doorway openings toward the two side exits while fire and smoke expand from the lower-central ignition source. At step 10, 4 agents have evacuated and smoke covers 89 cells; by step 20, 27 agents have evacuated and 3 fatalities have occurred. The snapshots show that furniture barriers, structural columns, and corridor access jointly shape route choice without producing the visual artefacts of an open-space obstacle mosaic.

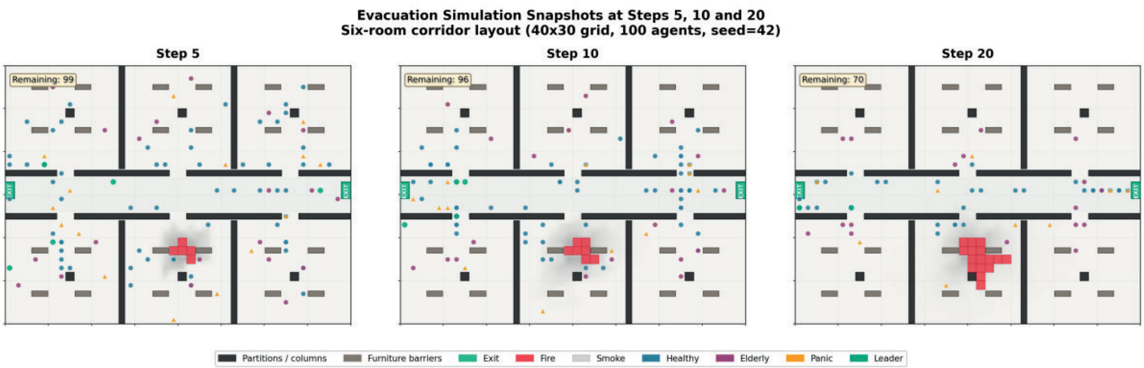

Figure 6. Evacuation snapshots at steps 5, 10, and 20 in the revised six-room corridor layout, showing agent positions, internal partitions, doorway openings, furniture barriers, structural columns, fire, and smoke

7. Multi-Metric Timeline Analysis

Figure 7 presents a comprehensive multi-metric timeline showing the simultaneous evolution of four key variables: remaining agents, evacuated agents, fire cells, and smoke cells.

Scientific Journal of Astana IT University
ISSN (P): 2707-9031 ISSN (E): 2707-904X
VOLUME 26, JUNE 2026

This integrated view reveals the dynamic interplay between evacuation progress and hazard propagation throughout the simulation.

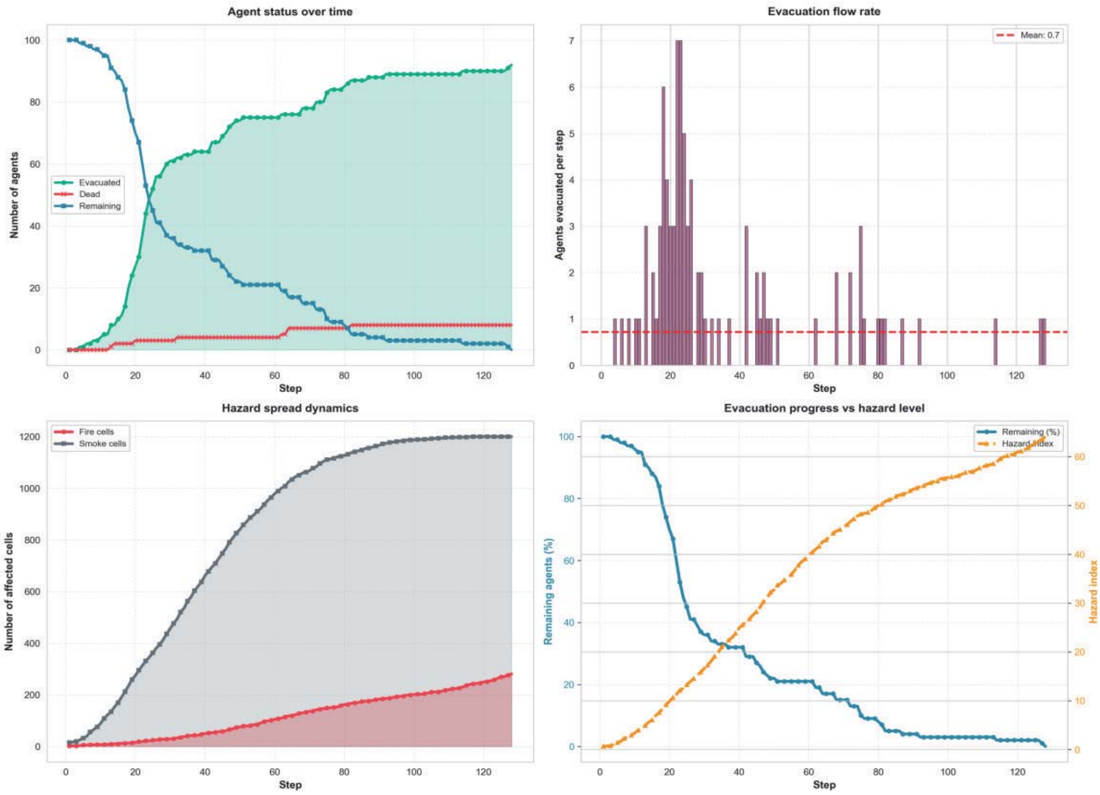

Figure 7. Four-metric timeline for the revised baseline run: remaining agents, cumulative evacuated agents, fire cells, and smoke cells

The decline in active agents is fastest during the main corridor-flow phase and slows after step 25, when the remaining population is composed mainly of elderly, panicking, or spatially isolated agents.

The cumulative evacuation curve rises to 92 agents and crosses the 50% threshold at step 25. This transition marks the shift from evacuation dominated by relatively accessible and mobile agents to a terminal phase governed by vulnerability, longer routes, and worsening smoke exposure.

Fire cells increase from 5 at step 5 to 16 at step 20 and reach 281 by step 128. Growth remains gradual during the peak evacuation interval, but the expanding fire front progressively reduces the set of safe route alternatives.

Smoke grows faster than fire and reaches full-grid saturation by step 128. Because smoke exposure reduces movement speed, its rapid expansion is central to late-stage evacuation performance even when fire occupies a smaller share of the grid.

Taken together, the timeline indicates tight coupling between evacuation progress and hazard development. By step 10, evacuation remains limited while smoke has already reached 89 cells; by step 25, 52 agents have evacuated and smoke has reached 362 cells. The revised baseline is therefore more demanding than the former open layout because partitions and furniture barriers delay part of the population while hazards continue to expand.

8. Statistical Summary

Table 4 provides descriptive statistics for evacuation/removal times by agent type. These values are used to compare the behavioural classes within the model and to provide reference points for future calibration, rather than to claim direct equivalence with measured evacuation times.

Table 4. Statistical summary of evacuation times by agent type (baseline run, seed = 42)

Agent type	**N**	**Mean**	**SD**	**Median**	**Range (steps)**
Healthy	60	29.6	19.4	23	4-82
Elderly	20	56.4	32.6	48	8-128
Panic	15	41.9	32.3	23	11-114
Leader	5	19.4	6.7	19	10-28
Overall	100	36.3	26.5	24	4-128

The revised baseline run ends at step 128 with 92 evacuated agents and 8 fatalities, corresponding to an evacuation rate of 0.92.

$$E = \frac{N_{evacuated}}{N_{total}} \tag{8}$$

These results still indicate substantial variability in individual evacuation times, driven primarily by differences in initial position, mobility, and hazard exposure. This reinforces the importance of considering delayed subpopulations rather than relying on aggregate averages alone.

The agent-type statistics reproduce the hierarchy observed in Figure 4: leaders (19.4 ± 6.7 steps), healthy adults (29.6 ± 19.4), panicking agents (41.9 ± 32.3), and elderly agents (56.4 ± 32.6). The 37.0-step gap between leaders and elderly agents demonstrates the extent to which mobility and behavioural assumptions shape late-stage outcomes.

Normalized variability reinforces this interpretation. Panicking agents have the highest coefficient of variation (0.77), reflecting stochastic route deviations, while leaders have the lowest value (0.35), reflecting deterministic navigation and greater visibility. Healthy and elderly agents occupy intermediate positions because their variability is driven primarily by starting location and exposure conditions.

Exit utilisation remains nearly balanced (48 versus 44), consistent with the symmetric side-exit configuration and the nearest-exit rule; the added partitions and furniture barriers do not produce a strong exit-use imbalance.

Hazard statistics further constrain interpretation: fire reaches 281 cells and smoke reaches 1200 cells by step 128, with smoke saturating the grid before all agents are removed.

9. Statistical Robustness (N = 30 Runs)

Stochastic robustness was assessed through 30 runs with seeds 1-30 and fixed model parameters. In the revised six-room corridor layout, the mean number of evacuated agents is 91.9 ± 4.3, mean fatalities are 8.1 ± 4.3, and mean completion time is 131.7 ± 16.0 steps. Every run ends with zero remaining active agents, indicating that the simulation horizon is sufficient for completion under the tested conditions.

Table 5. Summary statistics across 30 simulation runs (seed = 1–30)

Metric	**Mean**	**SD**	**Min**	**Max**
Evacuated	91.9	4.3	80	98
Dead	8.1	4.3	2	20
Steps to completion	131.7	16.0	81	158
Evacuation rate	0.919	0.043	0.800	0.980

Scientific Journal of Astana IT University
ISSN (P): 2707-9031 ISSN (E): 2707-904X
VOLUME 26, JUNE 2026

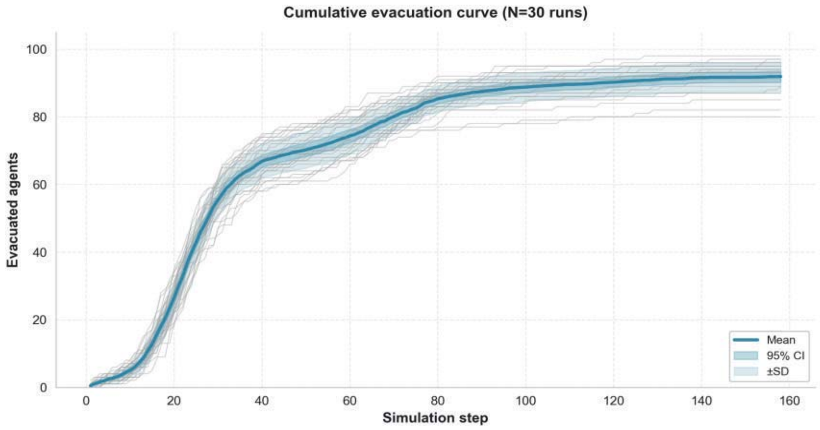

Figure 8. Mean cumulative evacuation curve across 30 runs (seeds 1-30) for the revised six-room corridor layout

10. Sensitivity Analysis

Fire spread probability was varied from 0.04 to 0.15, with 10 stochastic runs per value. The revised corridor-room geometry is sensitive to this parameter: mean evacuation rate declines from 0.955 at $p = 0.04$ to 0.854 at $p = 0.15$, while mean fatalities increase from 4.5 to 14.6. Faster fire spread therefore increases mortality in the constrained layout even though the exit configuration remains unchanged.

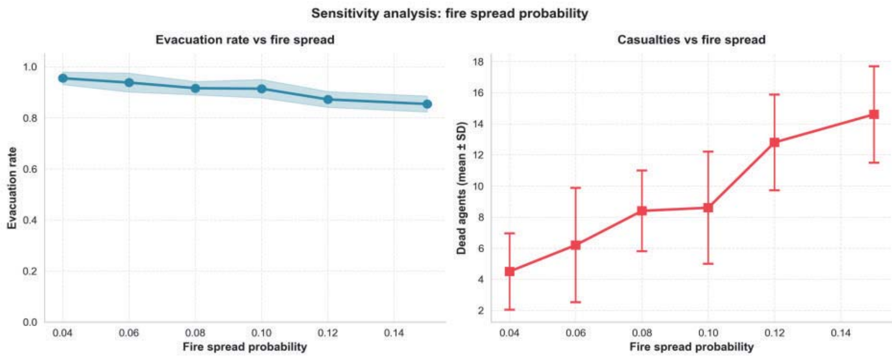

Figure 9. Sensitivity of evacuation rate and mean casualties to fire spread probability over $p = 0.04$-0.15

Discussion

1. Comparison with Literature Findings

The revised simulation is broadly consistent with recent evacuation-model findings, but the comparison must remain qualitative. The model is not calibrated to real seconds, and the 40×30 grid represents an abstract baseline rather than a measured building geometry. Literature comparisons are therefore used to assess plausibility of mechanisms, not numerical equivalence.

The elderly-agent speed reduction is consistent with empirical evidence that older evacuees and children move more slowly than healthy adults during emergencies [17]. The revised results show the same qualitative pattern, with elderly agents requiring substantially longer removal times than healthy adults, supporting the conclusion that vulnerable occupants can govern overall evacuation performance even when most agents leave earlier.

The hazard dynamics also align with the general finding that smoke can dominate evacuation risk before direct flame contact becomes widespread. In the revised run, smoke saturates the grid by the final step, while fire covers approximately 23.4% of cells. The 50% speed reduction in smoke-filled cells captures this mechanism in simplified form, but it should be read as an abstract mobility penalty rather than a physical prediction of smoke toxicity.

The balanced exit use in the simulation differs from empirical studies where familiarity, signage, and social influence can produce highly uneven exit selection [2]. Because the exit-selection rule assumes relatively good information about available exits, it may overestimate evacuation efficiency in real buildings, where visitors may follow others or choose familiar routes instead of geometrically shorter ones.

The leadership effect observed in the revised run is more modest than the 35% improvement reported for guided evacuation scenarios [8]. This discrepancy likely reflects differences in how leadership is implemented: our model treats leaders as individuals with superior visibility and deterministic pathfinding, whereas that work modeled leaders as actively guiding groups of followers [8]. The more substantial leadership effects reported there suggest that the primary benefit of trained personnel is not their individual performance but their ability to coordinate and guide others, a mechanism not captured in our current implementation.

Our fire spread algorithm, while simplified compared to full CFD simulations using FDS or PyroSim [5], captured essential dynamics of hazard propagation. FDS has been coupled with Pathfinder to analyze evacuation in bifurcated tunnels, calculating Fractional Effective Dose (FED) to assess survivability [5]. Our model does not currently implement FED calculations, representing a significant limitation for rigorous safety assessment. Future calibrated studies should integrate FED metrics to enable quantitative comparison with physics-based fire simulations and provide more robust survivability predictions.

2. Methodological Implications and Future Research Directions

The results offer methodological guidance rather than validated prescriptions for particular Astana buildings: under the present assumptions the configured layout supports distributed use of the two exits, but translating this into design guidance would require measured geometry, local regulatory context, and external validation.

The strong elderly–healthy gap indicates why vulnerable groups should be represented explicitly: a homogeneous population model would obscure the agents most likely to remain exposed during the terminal phase of evacuation.

The rapid smoke expansion in the revised run demonstrates the need to couple evacuation movement with smoke effects, even in a simplified grid model. Site-specific behavioural and geometric factors are not represented here and are left for future building-specific studies with access to local occupancy data.

The revised baseline run includes 8 fatalities, indicating that the scenario does not produce a complete no-loss evacuation. This outcome depends on several assumptions that may not hold in real emergencies: (1) immediate evacuation initiation without pre-movement delay, (2) perfect information about exit locations, (3) rational decision-making without panic-induced errors, and (4) moderate fire growth rates. Real evacuations often involve substantial pre-movement delays (30-120 seconds) as occupants assess the threat, gather belongings, and coordinate with others [20]. These limitations reinforce the need for caution when translating baseline-model outcomes into operational recommendations.

3. Model Limitations and Assumptions

Several limitations define the scope of interpretation. Although A* pathfinding prevents agents from crossing walls and produces obstacle-aware routes, the navigation model remains simpler than observed human behaviour. Agents are assumed to have relatively clear exit knowledge and to optimize individual routes, whereas real evacuees may act with incomplete information, follow social cues, or move as groups under stress [2]. Future versions should therefore incorporate familiarity-based exit choice, group following, and local crowd interactions, including social-force mechanisms where appropriate [9].

The fire and smoke algorithms are also simplified compared with physics-based tools such as FDS or Pathfinder. Reported times are abstract simulation steps, not real seconds, and should not be interpreted as physical estimates of evacuation duration or mortality risk. Heat transfer, combustion chemistry, and fluid dynamics are outside the present model. For the stated purpose

Scientific Journal of Astana IT University
ISSN (P): 2707-9031 ISSN (E): 2707-904X
VOLUME 26, JUNE 2026

of comparing relative behavioural outcomes under a controlled hazard, however, this abstraction is appropriate.

The model also does not currently implement pre-movement delays, which represent the time between alarm activation and evacuation initiation. Empirical studies show that pre-movement times typically range from 30-120 seconds and vary based on occupant activity, alarm type, and building familiarity [20]. Our simulation assumes immediate evacuation initiation (pre-movement time = 0), likely underestimating total evacuation times by 30-120 seconds. Future model versions should incorporate stochastic pre-movement delays drawn from empirically-calibrated distributions to provide more realistic evacuation time predictions.

The panic-behaviour implementation is also relatively simplistic, with panicking agents exhibiting a 30% probability of random movement. Real panic behavior is more complex, involving social influence, information seeking, and adaptive responses to perceived threats [20]. The proportion of panicking agents (15% in our model) is based on literature estimates rather than empirical data specific to Astana or Central Asian populations. Cultural factors, building familiarity, and prior emergency experience may influence panic prevalence and manifestation, requiring region-specific calibration.

Finally, the model does not account for several other real-world factors, including: (1) elevator usage and potential entrapment, (2) re-entry behavior where evacuees return to retrieve belongings or assist others, (3) communication and information sharing among agents, (4) physical disabilities beyond general mobility impairment, (5) carrying children or assisting others, and (6) visibility reduction from smoke affecting pathfinding. Each of these factors can significantly impact evacuation outcomes and should be considered in future model enhancements.

Beyond qualitative comparison, three behavioural parameters can be checked quantitatively against literature-reported ratios, without requiring the model to be calibrated to real seconds. The elderly-to-healthy speed ratio used here (0.5) falls within the range implied by combining reported healthy adult walking speeds of 1.2-1.4 m/s with reported elderly speeds of 0.5-0.8 m/s [25, 17], corresponding to a ratio of approximately 0.36-0.67. The modelled share of panicking agents (15%) lies within the 10-20% range reported for real evacuations [20]. The modelled 50% speed penalty in smoke-filled cells is consistent in direction and magnitude with the roughly 50% increase in evacuation time reported when smoke is explicitly modelled [11], noting that the two studies quantify different variables (instantaneous speed versus total time). Together with the agent-performance ordering, which is consistent with related agent-based evacuation studies [22, 25], these checks constitute a described, ratio-level comparison against the literature: stronger than face validity alone, though still short of calibration against a directly observed evacuation dataset. Empirical evacuation records specific to the modelled building type would be required for full calibration and formal validation.

Computational scale is another limitation. The current 100-agent, 40 × 30-grid scenario is tractable, but larger buildings, higher densities, or multi-floor evacuation would increase computational cost. Application to high-rise buildings would require additional model structure and may benefit from optimisation, parallel execution, or surrogate modelling [3].

Conclusion

This study presents a reproducible multi-agent evacuation simulation framework that couples stochastic fire and smoke propagation with heterogeneous agent behaviour in the open-source Mesa framework. The revised baseline run ends at step 128 with 92 evacuated agents and 8 fatalities, showing that agent heterogeneity, room-corridor geometry, and hazard growth jointly shape evacuation outcomes. The model should be read as a reproducible platform for comparative scenario analysis rather than as an operational prediction for a real building.

The timing of evacuation relative to hazard spread is central to this interpretation: smoke expands faster than the population can clear the corridor, so early warning, clear room-to-corridor access, and unobstructed paths to exits remain decisive within the assumptions of the model.

Beyond the specific numbers, the study contributes a transparent, reproducible workflow in which all figures, metrics, and narrative derive from a single consistent dataset; it demonstrates that comprehensive multi-agent evacuation models can be built on the accessible Mesa framework; and it identifies the assumptions that must be replaced before the framework can support building- and region-specific safety studies.

Future work should move the baseline toward calibrated and behaviourally richer evacuation modelling. Coupling with physics-based fire simulations such as FDS/PyroSim would allow more realistic hazard fields and survivability metrics such as Fractional Effective Dose, while behavioural extensions should include social-force interaction, group following, familiarity-based exit choice, pre-movement delay, re-entry behaviour, and communication. Integrating Kazakhstan building standards, measured floor plans, local occupancy data, and empirical evacuation records would turn the present abstract baseline into a practical benchmark for building-safety studies in Central Asia and other rapidly developing urban contexts.

References

[1] Wang, X., Liu, B., Ma, W., Feng, Y., Li, Q., & Sun, T. (2024). Simulations on evacuation strategy and evacuation process of the subway train under the fire. *Fire, 7*(12), 464. https://doi.org/10.3390/fire7120464

[2] Kasereka, S. K., Kalondji, N. E., Ilunga, G. W. K., Ngoie, R.-B. M., Kyamakya, K., & Kasoro, N. M. (2025). Enhancing building evacuation efficiency in case of fire breakout by integrating evacuee categorization into an agent-based simulation. *IEEE Access, 13*, 10595–10618. https://doi.org/10.1109/ACCESS.2025.3525480

[3] Senanayake, G. P. D. P., Kieu, M., Zou, Y., & Dirks, K. (2024). Agent-based simulation for pedestrian evacuation: A systematic literature review. *International Journal of Disaster Risk Reduction*. https://doi.org/10.1016/j.ijdrr.2024.104705

[4] Niu, L., & Song, Y. (2016). A simulation model fusing space and agent for indoor dynamic fire evacuation analysis. *Simulation, 92*(3), 215–232. https://doi.org/10.1177/0037549715626287

[5] Chen, J., Hu, Z., & Yang, S. (2024). Simulation of fire evacuation in a naturally ventilated bifurcated tunnel. *Fire, 7*(6), 202. https://doi.org/10.3390/fire7060202

[6] Alidmat, O. K. A., Umi, K. Y., Alhenawi, E., Badarneh, H. J., Alazaidah, R., & Al-Rbabah, L. (2023). Simulation of exit selection behavior evacuation based on an improved cellular automata model during fire disaster. *2023 24th International Arab Conference on Information Technology (ACIT)*, 1–8. https://doi.org/10.1109/ACIT58888.2023.10453699

[7] Alidmat, O. K. A., Alazaidah, R., Arabiat, M., Khafajeh, H., Aljaidi, M., Yusof, U. K., & Elrashidi, A. (2024). Dynamic exit selection and counting area adjustment for efficient crowd evacuation in asymmetrical layouts. *2024 25th International Arab Conference on Information Technology (ACIT)*, 1–10. https://doi.org/10.1109/ACIT62805.2024.10877032

[8] Zhang, P., Liu, W., Yang, L., Wu, J., Wang, K., & Cui, Y. (2025). A social force-based model for pedestrian evacuation with static guidance in emergency situations. *Fire, 8*(1), 30. https://doi.org/10.3390/fire8010030

[9] Ding, N., Zhu, Y., Liu, X., Dong, D., & Wang, Y. (2023). A modified social force model for crowd evacuation considering collision predicting behaviors. *Applied Mathematics and Computation*. https://doi.org/10.1016/j.amc.2023.128448

[10] Li, Z., Huang, H., Li, N., Chu, M. L., & Law, K. (2020). An agent-based simulator for indoor crowd evacuation considering fire impacts. *Automation in Construction*. https://doi.org/10.1016/j.autcon.2020.103395

[11] Jha, A., Lajnef, N., & Kodur, V. (2025). Modelling the effect of smoke on evacuation strategies in hospital buildings. *Buildings, 15*(17), 3093. https://doi.org/10.3390/buildings15173093

Scientific Journal of Astana IT University
ISSN (P): 2707-9031 ISSN (E): 2707-904X
VOLUME 26, JUNE 2026

[12] Zhang, W., Li, C., & Gai, W. (2024). How does evacuation risk change over time? Influences on evacuation strategies during accidental toxic gas releases. *International Journal of Disaster Risk Reduction*. https://doi.org/10.1016/j.ijdrr.2024.104531

[13] Song, H., Shi, Y., Yao, H., Wei, X., Qin, H., Lou, Z., Bai, Z., Li, J., & Yu, Y. (2024). Influence of wind direction on fire spread on high-rise building facades. *Fire, 7*(11), 384. https://doi.org/10.3390/fire7110384

[14] Liu, S., Liang, G., Shi, L., Luo, M., & Long, M. (2025). FDS-based study on fire spread and control in modern brick-timber architectural heritage: A case study of faculty house at a university in Changsha. *Sustainability, 17*(15), 6773. https://doi.org/10.3390/su17156773

[15] Lu, P., Zhang, Z., Onyebuchi, C. H., & Zheng, L. (2023). Agent-based modeling of high-rise building fires reveals self-rescue behaviors and better fire protection designs. *Engineering Applications of Artificial Intelligence*. https://doi.org/10.1016/j.engappai.2023.107401

[16] Tan, L., Hu, M., & Lin, H. (2014). Agent-based simulation of building evacuation: Combining human behavior with predictable spatial accessibility in a fire emergency. *Information Sciences*. https://doi.org/10.1016/j.ins.2014.09.029

[17] Chen, Y., Wang, C., Shen, Y., & Zhang, Y. (2025). A simulation-based method for the optimal building evacuation plan: A study of emergency behavior among older adults. Engineering, Construction and Architectural Management. Advance online publication. https://doi.org/10.1108/ECAM-11-2024-1558

[18] Chatra, M., & Bourahla, M. (2024). Agent-based simulation of crowd evacuation through complex spaces. *Ingénierie des Systèmes d'Information, 29*(1), 83–93. https://doi.org/10.18280/isi.290110

[19] Zhang, B., Lo, J. T. Y., Fang, H., Xie, C., Tang, T., & Lo, S. (2024). Coupled simulation-optimization model for pedestrian evacuation guidance planning. *Simulation Modelling Practice and Theory*. https://doi.org/10.1016/j.simpat.2024.102922

[20] Islas-Toski, M., Cuevas, E., Pérez-Cisneros, M., & Escobar, H. (2024). Agent-based evacuation modeling: Enhancing building safety in emergency scenarios. *Smart Cities, 7*(6), 3165–3187. https://doi.org/10.3390/smartcities7060123

[21] Xing, S., Wang, C., Wang, W., Cao, R. F., Yuen, A. C. Y., Lee, E. W. M., Yeoh, G. H., & Chan, Q. N. (2024). A fine discrete floor field cellular automaton model with natural step length for pedestrian dynamics. *Simulation Modelling Practice and Theory, 130*, 102841. https://doi.org/10.1016/j.simpat.2023.102841

[22] Zhang, Y., Li, W., Rui, Y., Wang, S., Zhu, H., & Yan, Z. (2022). A modified cellular automaton model of pedestrian evacuation in a tunnel fire. *Tunnelling and Underground Space Technology, 130*, 104673. https://doi.org/10.1016/j.tust.2022.104673

[23] Firdausyi, A. M., Dini, S. U., Nurafni, S., & Viridi, S. (2024). Pedestrian evacuation modeling using agent-based model and social-force model. *Journal of Physics: Conference Series, 2734*(1), 012032. https://doi.org/10.1088/1742-6596/2734/1/012032

[24] Wu, X., Zhang, L., Zhang, T., & Jiang, Q. (2025). Analysis of crowd vertical evacuation mechanism under different density conditions. *Physica A: Statistical Mechanics and its Applications, 657*, 130249. https://doi.org/10.1016/j.physa.2024.130249

[25] Giannoulaki, M., & Christoforou, Z. (2024). Pedestrian walking speed analysis: A systematic review. *Sustainability, 16*(11), 4813. https://doi.org/10.3390/su16114813

[26] Wei, X., Zhao, Y., Lian, L., Yao, H., Song, H., & Qin, H. (2023). Study on group movement characteristics in stairwell of high-rise buildings. *Buildings, 13*(1), 83. https://doi.org/10.3390/buildings13010083

[27] Yao, Y., Lu, W., & Wang, L. (2023). Experimental study on evacuation behaviour of children in a three-storey kindergarten. *Heliyon, 9*(6), e16533. https://doi.org/10.1016/j.heliyon.2023.e16533